

# A modular perspective to the jet suppression from a small to large radius in very high transverse momentum jets

Om Shahi,<sup>1</sup> Vaishnavi Desai,<sup>2</sup> and Prabhakar Palni<sup>2,\*</sup>

<sup>1</sup>*Department of Physics, BITS Pilani K. K. Birla Goa Campus, Goa.*

<sup>2</sup>*School of Physical & Applied Sciences, Goa University, Goa.*

In this work, we extend the scope of the JETSCAPE framework to cover the jet radius ( $R$ ) dependence of the jet nuclear modification factor,  $R_{AA}$ , for broader area jet cones, going all the way up to  $R = 1.0$ . The primary focus of this work has been the in-depth analysis of the high- $p_T$  inclusive jets and the quenching effects observed in the quark-gluon plasma formed in the Pb-Pb collisions at  $\sqrt{s_{NN}} = 5.02$  TeV for the most-central (0-10%) collisions. The nuclear modification factor is calculated for inclusive jets to compare with the experimental results collected at the ATLAS and the CMS detectors in the jet transverse momentum ( $p_T$ ) ranging from 100 GeV up to 1 TeV. The results predicted by the JETSCAPE are consistent in the high  $p_T$  range as well as for extreme jet cone sizes, i.e. within 10-20%. We also calculate the double ratio ( $R_{AA}^R/R_{AA}^{R=small}$ ) as a function of jet radius and jet- $p_T$ , where the observations are well described by the JETSCAPE framework which is based on the hydrodynamic multi-stage evolution of the parton shower. The calculations are then replicated for different low-virtuality based evolution models like the MARTINI and the AdS/CFT, which is followed by a rigorous comparison between the predictions from the former model combinations to the measurements at the CMS experiment.

## I. INTRODUCTION

The extremely hot and dense conditions created at the start of the big bang which we now understand as the soup of deconfined state of the partons, the quark-gluon plasma (QGP) [1–3]. The QGP is of such great interest that, to study the properties of this state of matter, particle physicists have spent decades building up the equipment which could recreate this extremely dense soupy state. The Relativistic Heavy-Ion Collider (RHIC) [4, 5] and the Large Hadron Collider (LHC) [6–9] conduct heavy-ion collisions where the QGP is created for very short instants of time, the parton shower propagation and modification are greatly influenced by the QGP medium. The high- $p_T$  jets produced in these heavy ion collisions undergo strong yield suppression and medium modification which are together referred to as jet quenching phenomena [10–12]. Therefore, we study the jet modification in nucleus-nucleus collisions relative to proton-proton collisions to probe the properties of the QGP via constraints from model-to-data comparison [13–16]. The measurement of the nuclear modification factor for jets as well as charged particles has revealed many important characteristics of the quark-gluon plasma [17–20]. It provides strong confirmation of the interaction of partons with the deconfined plasma, the respective medium modifications, and the eventual hydrodynamization with the medium [8]. Since there are many conclusive studies based on jet- $R_{AA}$  [21–25], our effort here is to push the limits of the current event generators and various energy loss modules for a better description of jet quenching phenomena at very high transverse momenta and broader jet cones with the multi-stage evolution of the parton shower

using the Jet Energy-loss Tomography with a Statistically and Computationally Advanced Program Envelope (JETSCAPE) framework (version 3.5.1) [26].

Along with these measurements, we study inclusive jet spectra for p-p and Pb-Pb by varying resolution parameters in the anti- $k_T$  algorithm which is realized in the FASTJET software package [27]. The inclusive jet spectrum is of significant interest because the sensitivity of hadronization effects is far less than the observables involving individual final-state hadrons. Here, the area of the reconstructed jet cone is defined by the jet radius  $R$ . Thus, by varying  $R$ , the reconstructed jet will include different proportions of energy from the medium response and the quenched jet. We also acknowledge the observations for a new sensitivity to QGP properties and underlying jet quenching mechanism in a study for jet yield suppression versus  $R$  [28]. Specifically, different dependences of the jet suppression on  $R$ , are predicted by theoretical models based on anti-de Sitter/conformal field theory correspondence [29] and perturbative QCD [30].

We begin with calculating the jet  $R_{AA}$  for the Pb-Pb collisions in Section II and compare with the experimental data from the ATLAS as well as the CMS detector for a robust test of configuration and the overall JETSCAPE framework. The calculations include the (2+1)D MUSIC [31] model for hydrodynamics which is ideal to study many aspects of heavy ion collisions. Most notably, this work covers the high- $p_T$  range of jets that is up to 1 TeV, which enables us to probe the QGP medium at much shorter distance scales.

We further exploit the advantages that the JETSCAPE framework offers in Section II A, that is the coupling of several different energy loss modules such as MARTINI [32] and AdS/CFT [33] with the MATTER [34] module to explore the quenching effects in a multi-stage manner. This approach provides insight into the interaction and energy loss mechanism in the

\* Corresponding author: [prabhakar.palni@unigoa.ac.in](mailto:prabhakar.palni@unigoa.ac.in)

medium with respect to the virtuality of the partonic jet. Comparing the experimental data with the trends from these different models which handle the low virtuality phase allows us to develop a lucid understanding of the physics governing the above models.

In Section II B, we proceed with concrete results from the above combinations of several successful models towards the jet radius dependence studies. An important measurement done by the CMS collaboration recently was the jet- $R_{AA}$  for Pb-Pb collisions at the LHC and recording the data for jet cone area covering the radii from 0.2 up to 1 [35]. This analysis gives us an intricate understanding of the behaviour and interaction strength of the high- $p_T$  inclusive collimated jets in proximity to the jet axis, for  $R = 0.2$  and the energy distribution around the cone for values of radii up to 1. The current JETSCAPE framework is based on calculations of perturbative QCD and evolution in a dense medium, thus allowing us to go up to a radius of order 1. We also report the ratios of  $R_{AA}$  for a given  $R$  with respect to  $R = 0.2$  as a function of jet- $p_T$  and jet radius  $R$ . This study provides a vivid picture of the energy transactions with the QGP as the jet cone size increases and the trends that the JETSCAPE framework predicts.

We conclude this work in Section III, with a concise account of the current JETSCAPE framework's potential to explain the jet- $R_{AA}$  for larger area jet cones. We also shed light on the ability of the distinct combination of modules to describe the jet- $R_{AA}$ .

### A. SIMULATION WITH MULTI-STAGE ENERGY LOSS PERSPECTIVE IN JETSCAPE

The JETSCAPE framework provides an ideal environment for carrying out multi-stage energy loss. The hard scattering is generated by PYTHIA 8 [36] with initial state radiation (ISR) and multiparton interaction (MPI) [37] turned on, and final state radiation (FSR) turned off. For the event wise simulations, the TRENTo model [38] sets up the initial conditions and the viscous hydrodynamic evolution is described by the (2+1)D MUSIC [31] model followed by Cooper-Frye prescription [39, 40] which converts the fluid cells to hadrons on an isothermal hypersurface [41] at  $T_{SW} = 151$  MeV, where  $T_{SW}$  is the temperature of the plasma below which particlization [42] occurs at a certain hypersurface. The jet energy loss induced by scattering is calculated in a succession of two stages: MATTER [34, 43] which takes care of the highly virtual phase (the first stage) while the low virtuality phase (the second stage), is handled concurrently by the LBT model [44–46]. We have also employed the MARTINI [32, 47, 48] and the AdS/CFT model [33] in combination with the MATTER model to explore the low virtuality phase. The virtuality of the parton is defined as  $Q^2 = p^\mu p_\mu - m^2$ . The parton undergoes energy loss in two stages, when the virtuality of the parton,  $Q^2 > Q_{SW}^2$ , where  $Q_{SW}$  is the switching virtuality, the

MATTER model handles the energy loss and the parton is transferred to the LBT model once  $Q^2 \leq Q_{SW}^2$ . In these calculations, the jet medium interaction includes inelastic medium-induced gluon radiation and a medium recoil. An extensive account of the comparison of the model to the existing jet- $R_{AA}$  is already done [49], showing that the contribution of medium recoil is quite significant in the modification of jet- $R_{AA}$  for a complete set of centrality classes ranging from the most central collisions to the peripheral collisions. This version of the JETSCAPE framework [26] encompasses the modifications of a hard thermal-loop (HTL) [50] for fixed coupling ( $\alpha_s^{\text{fix}}$ ), running coupling ( $\alpha_s$ ), and with a virtuality dependent factor,  $f(Q^2)$ , that modulates the effective value of jet transport coefficient ( $\hat{q}$ ). It also accounts for the reduced medium-induced emission in the high virtuality phase, due to coherence effects. The calculations based on the Hard Thermal Loop (HTL) considering weak-coupling approximation and the limits of high-temperature yield for a  $\hat{q}$  is given as [45],

$$\hat{q}_{\text{HTL}} = C_a \frac{42\zeta(3)}{\pi} \alpha_s^2 T^3 \ln \left[ \frac{ET}{3\pi T^2 \alpha_s^{\text{fix}}} \right]. \quad (1)$$

where  $C_a$  is the representation specific Casimir,  $E$  is the energy of the hard parton, and  $T$  is the local temperature of the medium. The coherence effects which reduce the interaction strength of the parton with the medium are also taken into consideration as the virtuality-dependent modulation factor, which regulates the effective value of  $\hat{q}$  in the high virtuality MATTER event generator. The parameterization of the virtuality-dependent modulation factor is given as [49]

$$\hat{q} \cdot f \equiv \hat{q}_{\text{HTL}}^{\text{run}} f(Q^2), \quad (2)$$

$$f(Q^2) = \begin{cases} \frac{1+10 \ln^2(Q_{sw}^2)+100 \ln^4(Q_{sw}^2)}{1+10 \ln^2(Q^2)+100 \ln^4(Q^2)} & Q^2 > Q_{sw}^2 \\ 1 & Q^2 \leq Q_{sw}^2 \end{cases} \quad (3)$$

here  $Q^2$  is the running virtuality of the hard parton. Finally, the partons undergo colorless hadronization according to the default Lund string fragmentation from PYTHIA 8 [36, 51]. The contributions in final jets are from the hard jet shower part and the effect from the soft medium response, the latter is calculated via the Cooper-Frye formula [39, 40]. We reconstruct jets for several radius selections using the anti- $k_T$  algorithm which is realized in the FASTJET and compare with experimental data. The Underlying Events (UE) [52, 53] are removed by implementing a minimum track requirement of  $p_T^{\text{track, min}} > 4$  GeV. All the parameters involved in the tuning of the constituent modules follow the standard set of tunes released by the JETSCAPE Collaboration in an elaborate recent study [49].

## II. RESULTS

This work covers the collision energy:  $\sqrt{s_{NN}} = 5.02$  TeV for the most central (0-10%) Pb-Pb collisions and

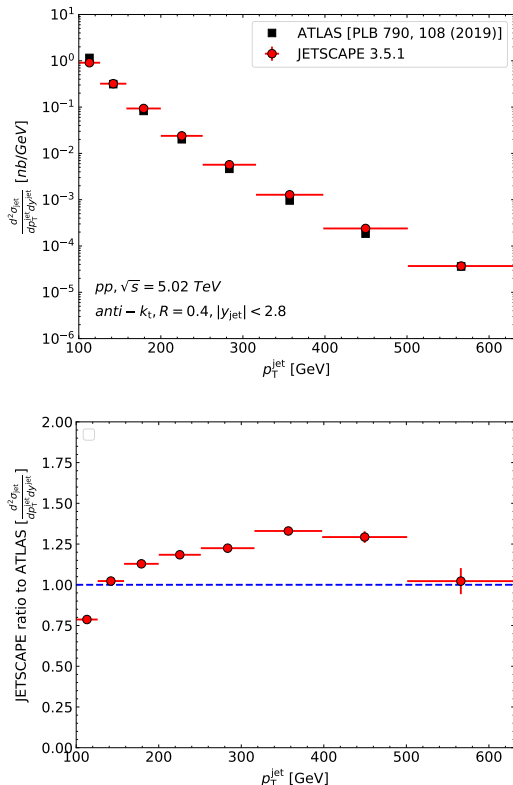


FIG. 1. (Color online) Differential cross-section of inclusive jets for  $p+p$  collisions with cone size  $R=0.4$ , with a minimum track requirement of  $p_T^{\text{track}} > 4$  GeV. Bottom panel shows the JETSCAPE ratio to the ATLAS data.

shows a comparison with selected experimental data available from the ATLAS and the CMS collaborations. The energy loss depicted in this work is achieved by the coupling of MATTER with LBT module. The secondary LBT module (which handles the low virtuality phase) remains the same throughout until and unless specified. Fig. 1 (top panel) shows the  $p+p$  collision results for inclusive jet spectra at  $\sqrt{s} = 5.02$  TeV for  $|y_{jet}| < 2.8$ , which follow the JETSCAPE PP-19 tune [54], are then compared to the experimental data from the ATLAS [24, 25]. The ratio of inclusive jet cross-section using the JETSCAPE to the ATLAS data is shown in the bottom panel of Fig. 1, which shows that the results are in the acceptable range up to ( $\leq 20 - 30\%$ ). We report the 0-10% most central Pb-Pb jet spectra for  $R = 0.4$  in Fig. 2. The ratio of the differential cross-section for inclusive jets in Pb-Pb collisions using JETSCAPE to the ATLAS [25] data are shown in Fig. 2. Here,  $R_{AA}$  is defined as

$$R_{AA} = \frac{1}{N_{evt}} \frac{d^2 N_{jet}}{dy_{jet} dp_T^{\text{jet}}} \Big|_{AA}, \quad (4)$$

$$\frac{d^2 \sigma_{jet}}{dy_{jet} dp_T^{\text{jet}}} \Big|_{pp}$$

Where  $\sigma_{jet}$  and  $N_{jet}$  are the inclusive jet cross-section in  $p+p$  collisions and the jet yield in Pb+Pb collisions,

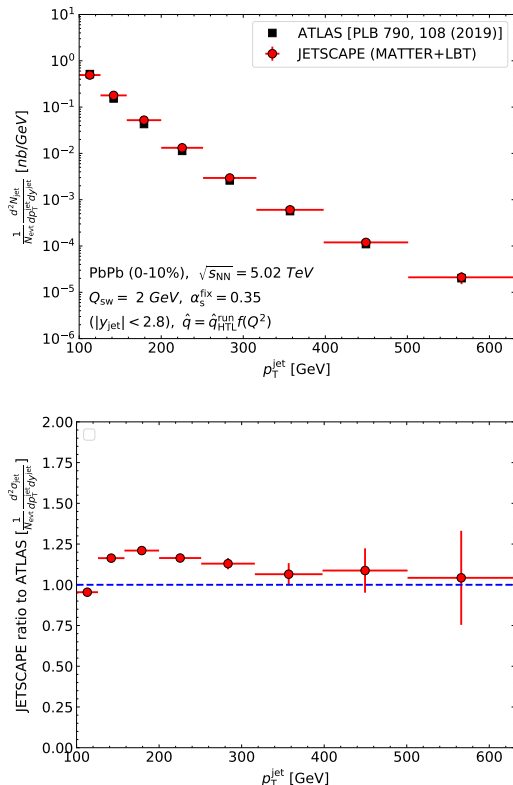


FIG. 2. Differential cross-section of inclusive jets in Pb+Pb collisions at  $\sqrt{s_{NN}} = 5.02$  TeV with cone size  $R = 0.4$ , with a minimum track requirement of  $p_T^{\text{track}} > 4$  GeV. Bottom panel shows the ratio of the JETSCAPE to the ATLAS data.

respectively, which are measured as a function of transverse momentum,  $p_T$ , and rapidity,  $y$ . Moreover,  $N_{evt}$  is the number of Pb+Pb collisions within a specific rapidity interval. The inclusive jet- $R_{AA}$  is calculated as the ratio of the Pb-Pb and p-p spectra, which is shown in Fig. 3 in comparison to the ATLAS data. The JETSCAPE (MATTER + LBT) results agree with the ATLAS data quite nicely. However, we see an enhancement ( $\leq 10 - 20\%$ ) in the low  $p_T$  region below 180 GeV, which is followed by marginal suppression above 300 GeV, as we ascend in the  $p_T$  range.

#### A. Exploring the MARTINI and AdS/CFT models

Both the MARTINI [32] and the AdS/CFT [33] models are designed to handle the low virtuality phase and carry forward the energy loss once the parton is transferred from the MATTER. We replace the successful LBT model with the MARTINI, to carry out the simulations for the same conditions [49] and compare the jet- $R_{AA}$  with the experimental data from the ATLAS [25] and the CMS [35] collaboration. Similarly, the calculations are done by replacing the LBT with AdS/CFT model and compared with the experimental data.

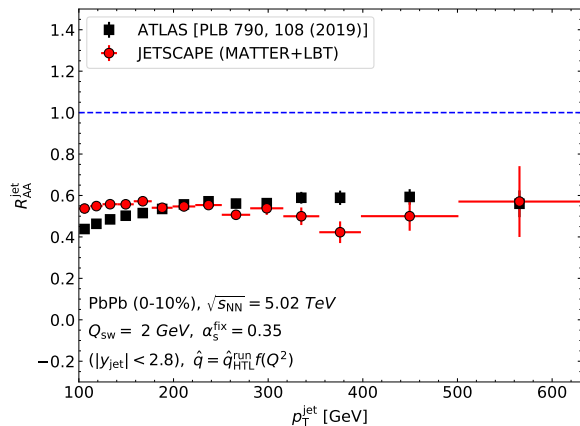


FIG. 3. (Color online) the jet- $R_{AA}$  as a function of jet- $p_T$  for inclusive jets in the most central (0-10%) Pb+Pb collisions at  $\sqrt{s_{NN}} = 5.02$  TeV for the jet cone radius  $R = 0.4$ .

We further present the intensive comparison between the low virtuality parton evolution models, where the inclusive jet- $R_{AA}$  is calculated for three models, MATTER coupled with LBT (which is our default), MATTER coupled with MARTINI, and MATTER coupled with AdS/CFT. The simulations are altogether staged in contrast with the experimental data from the CMS [35], for Pb-Pb collisions at  $\sqrt{s_{NN}} = 5.02$  TeV and for a range of jet cone sizes up to an order of 1 and  $p_T^{jet}$  range up to 1 TeV.

The measurements for different models are now manifest in Fig. 4, which shows the jet- $R_{AA}$  for  $|y_{jet}| < 2$  and jet cone radius  $R = 0.2$ , in comparison with the experimental data from the CMS Collaboration [35]. Similarly, Fig. 4 shows the jet- $R_{AA}$  which is also measured for  $R = 0.3$ ,  $R = 0.4$ ,  $R = 0.6$ ,  $R = 0.8$ , and  $R = 1.0$  over a range of jet- $p_T$  from 300 GeV up to 1 TeV. The predictions made by the JETSCAPE are consistent even as we advance to the larger area jet cones. The JETSCAPE predicts marginally more suppression from a small to intermediate to large radius for all the modular combinations discussed above. The results predicted by the (MATTER + LBT) and (MATTER + MARTINI) are congruous with the experimental observations throughout the  $p_T$  range and across the different jet radii. While the (MATTER + AdS/CFT) model shows more suppression in the intermediate  $p_T$  and significant enhancement at high  $p_T$  region as compared to the other modular combinations. At very high transverse momentum, the virtuality of the dominant partons is very high and due to the coherence effects, the interaction strength of the parton with the medium is significantly reduced. Since the radiative energy loss in AdS/CFT is more dominant than the elastic jet energy loss as compared to LBT and MARTINI, there is a considerable enhancement of jet- $R_{AA}$  in the high  $p_T$  due to the minimized elastic jet energy loss. Also, the effect of the recoil partons in LBT on the total

energy loss is not very significant. It is very articulate that there is an appreciable reduction in net elastic and radiative jet energy loss when the jet cone includes the recoil partons.

With the above comparisons to both ATLAS and CMS experimental data (Fig. 1-4), the results from the JETSCAPE are substantially credible for further jet radius-dependent investigations using the current models, which is carried out in the next section.

## B. Jet radius ( $R$ ) and jet- $p_T$ dependence of the $R_{AA}$

In this section, we emphasize the significant contribution from the hydrodynamic medium response already highlighted in previous studies [8, 55], which is observed in the jet- $R_{AA}$  as a function of jet radius. Through radius-dependent studies, we develop a clear picture of the role played by radiation and collisions in energy loss.

A recent study by the CMS collaboration [35] enlightens the rigorous comparisons of predictions from quenched jet event generators like HYDJET++ [56], PYQUEN [57] and theoretical models used to replicate relativistic heavy ion collisions to the experimental data for the jet- $R_{AA}$ . The article concludes with the impression that although most state-of-the-art models have progressed, significant uncertainty remains for the large-area jets.

The large jet radius also implies that the jet retains a significant proportion of the extensively distributed momentum and energy deposited in the plasma. Since the JETSCAPE framework has pioneered the realization of a multi-stage approach for modular-based energy loss, the motivation here is to challenge the JETSCAPE model that has so far met our expectations in describing the variety of data observed and to investigate the limitations of the current models.

This quest is executed by calculating the jet- $R_{AA}$  double ratio ( $R_{AA}^R/R_{AA}^{R=0.2}$ ) and as a function of jet radius which is in comparison with the CMS data for the most central (0-10%) Pb-Pb collisions over a range of jet- $p_T$  from 300 GeV up to 1 TeV. The plots are further sub-categorized by three jet- $p_T$  intervals.

For  $300 \text{ GeV} \leq p_{T,jet} \leq 400 \text{ GeV}$ , Fig. 5 (left panel) shows the predictions by the different combination of energy loss models. We observe a consistent trend for all three models, i.e. (MATTER + LBT), (MATTER + MARTINI), and (MATTER + AdS/CFT). The results are within the uncertainty limits. The trend predicted by all three modular combinations with a different low-virtuality handling model is pretty similar to a considerable extent. This also indicates that the energy loss of the partons in the intermediate  $p_T$  range throughout the various jet cone sizes is comparable among LBT, MARTINI, and AdS/CFT.

For  $400 \text{ GeV} \leq p_{T,jet} \leq 500 \text{ GeV}$ , in Fig. 5 (center panel), we observe that (MATTER + LBT) is in fine agreement with the data while both (MATTER + MAR-



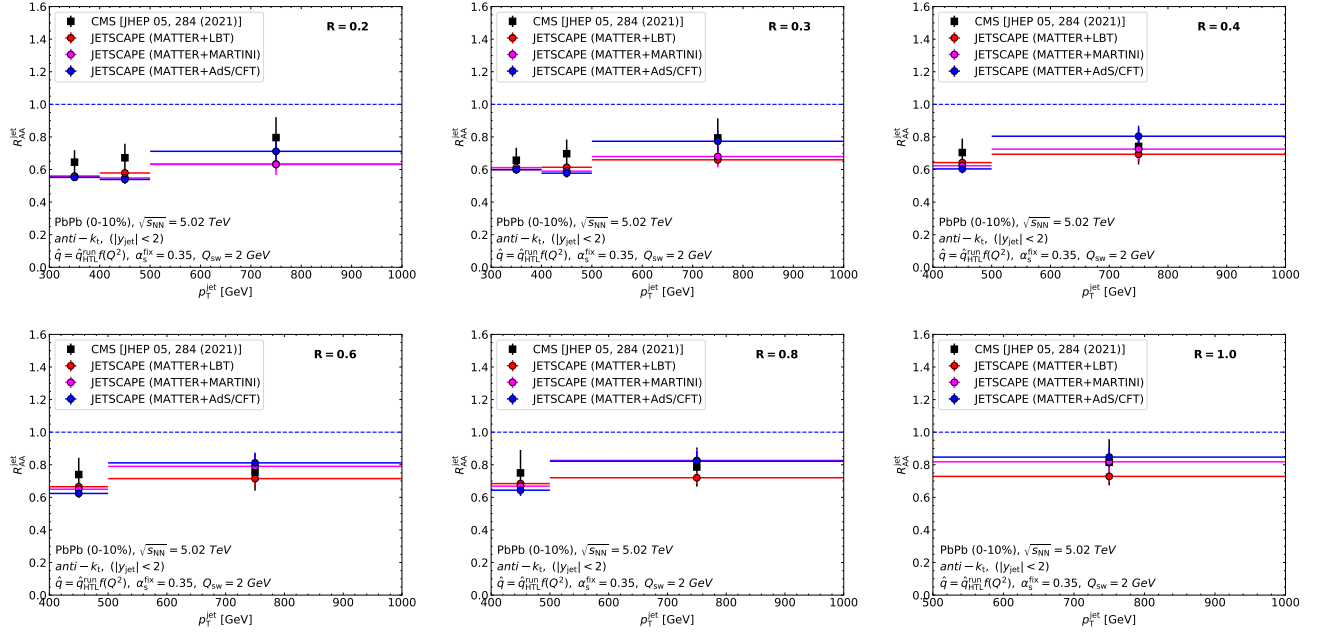


FIG. 4. The jet- $R_{AA}$  as a function of jet- $p_T$  for inclusive jets in the most central (0-10%) Pb+Pb collisions at  $\sqrt{s_{NN}} = 5.02$  TeV for the jet cone radius  $R = 0.2, 0.3, 0.4, 0.6, 0.8$  and  $1.0$  with  $|y_{jet}| < 2$  and a minimum track requirement of  $p_T^{\text{track}} > 4$  GeV. The plot shows the comparison between the models by red, magenta, and blue markers for (MATTER + LBT), (MATTER + MARTINI), and (MATTER + AdS/CFT), respectively. The predictions are in comparison with CMS data shown with a black marker.

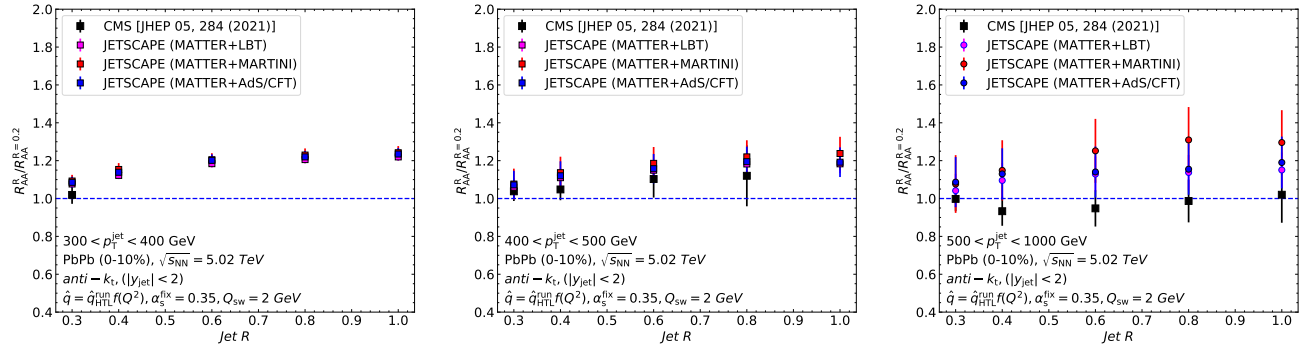


FIG. 5. The double ratio ( $R_{AA}^R/R_{AA}^{R=0.2}$ ) as a function of jet radius for inclusive jets for ( $300 \text{ GeV} \leq p_{T,jet} \leq 400 \text{ GeV}$ ) (left panel), ( $400 \text{ GeV} \leq p_{T,jet} \leq 500 \text{ GeV}$ ) (centre panel), and ( $500 \text{ GeV} \leq p_{T,jet} \leq 1 \text{ TeV}$ ) (right panel), in the most central (0-10%) Pb+Pb collisions at  $\sqrt{s_{NN}} = 5.02$  TeV for different jet radii with  $|y_{jet}| < 2$  and a minimum track requirement of  $p_T^{\text{track}} > 4$  GeV. The plot shows the comparison between the models by magenta, red and blue markers for (MATTER+LBT), (MATTER+MARTINI), and (MATTER+AdS/CFT), respectively. The predictions are in comparison with CMS data shown with a black marker.

TINI) and (MATTER + AdS/CFT), tend to slightly over-predict the jet- $R_{AA}$  ( $\leq 15\%$ ).

In the extreme high  $p_{T,jet}$  region, that is for  $500 \text{ GeV} \leq p_{T,jet} \leq 1 \text{ TeV}$ , in Fig. 5 (right panel), shows that all the models significantly over-predict the jet- $R_{AA}$ , with the best description provided by the (MATTER + LBT) model ( $\leq 20\%$ ). All the models show saturation around jet radius  $R = 0.8$  and  $R = 1.0$ , which fits well for a realistic approach. Altogether, the JETSCAPE framework nicely describes the full evolution of the par-

ton shower by adopting a virtuality-based multi-stage approach for energy loss.

We also measure the jet- $R_{AA}$  double ratio ( $R_{AA}^R/R_{AA}^{R=0.2}$ ) as a function of jet- $p_T$  in Fig. 6. We observe that as the jet is scattered in the medium, the final state partons of the medium interacting with the jet are also considered a constituent of the jet. As more and more gluons fall into the larger jet cone and prohibit from contributing to the jet energy loss. Therefore, energy lost by the jets is partially gained as

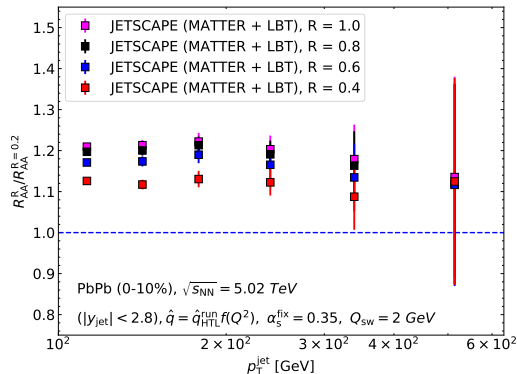


FIG. 6. The double ratio ( $R_{AA}^R/R_{AA}^{R=0.2}$ ) as a function of jet- $p_T$  for inclusive jets in the most central (0-10%) Pb+Pb collisions at  $\sqrt{s_{NN}} = 5.02$  TeV for different jet radii with  $|y_{jet}| < 2.8$ .

the area of the jet cone increases. Here we observe a non-monotonous rise in the double ratio for jet- $p_T \leq 200$  GeV, followed by a fall in the intermediate  $p_T$  to high  $p_T$  region.

### III. CONCLUSION

In this paper, we present the comparisons of the jet- $R_{AA}$  predictions from the JETSCAPE framework incorporating the (2+1)D MUSIC model for viscous hydrodynamic evolution to the ATLAS data for Pb+Pb collisions at  $\sqrt{s_{NN}} = 5.02$  TeV in high jet transverse momentum interval  $100 \text{ GeV} \leq p_{T,jet} \leq 1 \text{ TeV}$  for anti- $k_T$  jets of radius  $R=0.4$ . These results put us in a strong stance to conclude that the MUSIC model is adequate and also successful in speculating the experimental observations

even at higher jet- $p_T$  for the most central collisions as well as mid-central collisions.

This work also elucidates the predictions made by low virtuality-based evolution models like MARTINI and AdS/CFT in a hydrodynamic medium generated by the MUSIC. We observe overall similar trend anticipations as compared to the unfolding in other hydrodynamic models like (2+1)D VISHNU [58]. The MUSIC model is less sensitive to coherence effects which are prevalent at high transverse momentum, compared to VISHNU. We observe more suppression in the intermediate and extreme  $p_T$  regions, which provides a better description of the observed data ( $\leq 15\%$ ).

We advance the current JETSCAPE calculations and compare with the data of wider jet cones ranging from  $R = 0.2$  to  $R = 1.0$  recorded at the CMS detector for Pb+Pb collisions at  $\sqrt{s_{NN}} = 5.02$  TeV in high jet transverse momentum interval  $300 \text{ GeV} \leq p_{T,jet} \leq 1 \text{ TeV}$  for anti- $k_T$  jets of radii  $R = 0.2, 0.3, 0.4, 0.6, 0.8,$  and  $1.0$ . Although the JETSCAPE framework is still under improvisation to define the jet medium interactions at wide angles, this work highlights the current standing of the model to describe the energy loss and medium response phenomenon for broad area jet cones.

### IV. ACKNOWLEDGEMENTS

We express our gratitude to the JETSCAPE Collaboration for making the state-of-the-art framework publicly available for extensive research use. The authors would like to especially acknowledge the members of the JETSCAPE Collaboration, Yasuki Tachibana and Chun Shen for their useful discussion and valuable feedback. The authors would also like to thank Goa University Param computing facility, SPAS local cluster facility, and seed money grant support.

- 
- [1] P. B. Arnold, G. D. Moore, and L. G. Yaffe, Photon and gluon emission in relativistic plasmas, *JHEP* **06**, 030, [arXiv:hep-ph/0204343](#).
  - [2] P. B. Arnold, G. D. Moore, and L. G. Yaffe, Photon emission from ultrarelativistic plasmas, *JHEP* **11**, 057, [arXiv:hep-ph/0109064](#).
  - [3] Z. Yang, T. Luo, W. Chen, L.-G. Pang, and X.-N. Wang, 3D structure of jet-induced diffusion wake in an expanding quark-gluon plasma, (2022), [arXiv:2203.03683 \[hep-ph\]](#).
  - [4] I. P. Lokhtin and A. M. Snigirev, A Model of jet quenching in ultrarelativistic heavy ion collisions and high-p(T) hadron spectra at RHIC, *Eur. Phys. J. C* **45**, 211 (2006), [arXiv:hep-ph/0506189](#).
  - [5] S. Cao, T. Luo, G.-Y. Qin, and X.-N. Wang, Heavy and light flavor jet quenching at RHIC and LHC energies, *Phys. Lett. B* **777**, 255 (2018), [arXiv:1703.00822 \[nucl-th\]](#).
  - [6] R. B. Neufeld and I. Vitev, Parton showers as sources of energy-momentum deposition in the QGP and their implication for shockwave formation at RHIC and at the LHC, *Phys. Rev. C* **86**, 024905 (2012), [arXiv:1105.2067 \[hep-ph\]](#).
  - [7] F. Ringer, B.-W. Xiao, and F. Yuan, Can we observe jet  $P_T$ -broadening in heavy-ion collisions at the LHC?, *Phys. Lett. B* **808**, 135634 (2020), [arXiv:1907.12541 \[hep-ph\]](#).
  - [8] N.-B. Chang, Y. Tachibana, and G.-Y. Qin, Nuclear modification of jet shape for inclusive jets and  $\gamma$ -jets at the LHC energies, *Physics Letters B* **801**, 135181 (2020).
  - [9] A. Luo, Y.-X. Mao, G.-Y. Qin, E.-K. Wang, and H.-Z. Zhang, Jet shape and redistribution of the lost energy from jets in Pb + Pb collisions at the LHC in a multiphase transport model, *Eur. Phys. J. C* **82**, 156 (2022), [arXiv:2107.11751 \[hep-ph\]](#).
  - [10] M. Gyulassy, P. Levai, and I. Vitev, Jet quenching in thin quark gluon plasmas. 1. Formalism, *Nucl. Phys. B* **571**,

- 197 (2000), [arXiv:hep-ph/9907461](#).
- [11] G.-Y. Qin and X.-N. Wang, Jet quenching in high-energy heavy-ion collisions, *Int. J. Mod. Phys. E* **24**, 1530014 (2015), [arXiv:1511.00790 \[hep-ph\]](#).
- [12] S. Cao and X.-N. Wang, Jet quenching and medium response in high-energy heavy-ion collisions: a review, *Rept. Prog. Phys.* **84**, 024301 (2021), [arXiv:2002.04028 \[hep-ph\]](#).
- [13] D. A. Appel, Jets as a Probe of Quark - Gluon Plasmas, *Phys. Rev. D* **33**, 717 (1986).
- [14] R. Baier, Y. L. Dokshitzer, A. H. Mueller, S. Peigne, and D. Schiff, Radiative energy loss of high-energy quarks and gluons in a finite volume quark - gluon plasma, *Nucl. Phys. B* **483**, 291 (1997), [arXiv:hep-ph/9607355](#).
- [15] R. Baier, Y. L. Dokshitzer, A. H. Mueller, S. Peigne, and D. Schiff, Radiative energy loss and p(T) broadening of high-energy partons in nuclei, *Nucl. Phys. B* **484**, 265 (1997), [arXiv:hep-ph/9608322](#).
- [16] B. G. Zakharov, Fully quantum treatment of the Landau-Pomeranchuk-Migdal effect in QED and QCD, *JETP Lett.* **63**, 952 (1996), [arXiv:hep-ph/9607440](#).
- [17] G. Aad *et al.* (ATLAS), Measurement of inclusive jet charged-particle fragmentation functions in Pb+Pb collisions at  $\sqrt{s_{NN}} = 2.76$  TeV with the ATLAS detector, *Phys. Lett. B* **739**, 320 (2014), [arXiv:1406.2979 \[hep-ex\]](#).
- [18] G. Aad *et al.* (ATLAS), Measurement of angular and momentum distributions of charged particles within and around jets in Pb+Pb and *pp* collisions at  $\sqrt{s_{NN}} = 5.02$  TeV with the ATLAS detector, *Phys. Rev. C* **100**, 064901 (2019), [Erratum: *Phys.Rev.C* 101, 059903 (2020)], [arXiv:1908.05264 \[nucl-ex\]](#).
- [19] J. Adam *et al.* (STAR), Measurement of inclusive charged-particle jet production in Au + Au collisions at  $\sqrt{s_{NN}} = 200$  GeV, *Phys. Rev. C* **102**, 054913 (2020), [arXiv:2006.00582 \[nucl-ex\]](#).
- [20] S. S. Adler *et al.* (PHENIX), High  $p_T$  charged hadron suppression in Au + Au collisions at  $\sqrt{s_{NN}} = 200$  GeV, *Phys. Rev. C* **69**, 034910 (2004), [arXiv:nucl-ex/0308006](#).
- [21] ATLAS Collaboration, Measurement of substructure-dependent jet suppression in pb+pb collisions at 5.02 tev with the atlas detector (2022).
- [22] A. M. Sirunyan *et al.* (CMS), In-medium modification of dijets in PbPb collisions at  $\sqrt{s_{NN}} = 5.02$  TeV, *JHEP* **05**, 116, [arXiv:2101.04720 \[hep-ex\]](#).
- [23] G. Aad *et al.* (ATLAS), Measurement of the jet radius and transverse momentum dependence of inclusive jet suppression in lead-lead collisions at  $\sqrt{s_{NN}} = 2.76$  TeV with the ATLAS detector, *Phys. Lett. B* **719**, 220 (2013), [arXiv:1208.1967 \[hep-ex\]](#).
- [24] M. Aaboud *et al.* (ATLAS), Measurement of the nuclear modification factor for inclusive jets in Pb+Pb collisions at  $\sqrt{s_{NN}} = 5.02$  TeV with the ATLAS detector, *Phys. Lett. B* **790**, 108 (2019), [arXiv:1805.05635 \[nucl-ex\]](#).
- [25] Measurement of substructure-dependent jet suppression in Pb+Pb collisions at 5.02 TeV with the ATLAS detector, (2022), [arXiv:2211.11470 \[nucl-ex\]](#).
- [26] J. H. Putschke *et al.*, The JETSCAPE framework, (2019), [arXiv:1903.07706 \[nucl-th\]](#).
- [27] M. Cacciari, G. P. Salam, and G. Soyez, FastJet User Manual, *Eur. Phys. J. C* **72**, 1896 (2012), [arXiv:1111.6097 \[hep-ph\]](#).
- [28] Y.-T. Chien and I. Vitev, Towards the understanding of jet shapes and cross sections in heavy ion collisions using soft-collinear effective theory, *Journal of High Energy Physics* **2016**, 10.1007/jhep05(2016)023 (2016).
- [29] Z. Hulcher, D. Pablos, and K. Rajagopal, Resolution effects in the hybrid strong/weak coupling model, *Journal of High Energy Physics* **2018**, 10.1007/jhep03(2018)010 (2018).
- [30] N. Armesto, L. Cunqueiro, and C. A. Salgado, Q-PYTHIA: a medium-modified implementation of final state radiation, *The European Physical Journal C* **63**, 10.1140/epjc/s10052-009-1133-9 (2009).
- [31] B. Schenke, S. Jeon, and C. Gale, (3+1)d hydrodynamic simulation of relativistic heavy-ion collisions, *Physical Review C* **82**, 10.1103/physrevc.82.014903 (2010).
- [32] B. Schenke, C. Gale, and S. Jeon, MARTINI: An Event generator for relativistic heavy-ion collisions, *Phys. Rev. C* **80**, 054913 (2009), [arXiv:0909.2037 \[hep-ph\]](#).
- [33] J. L. Albacete, Y. V. Kovchegov, and A. Taliotis, Modeling heavy ion collisions in AdS/CFT, *Journal of High Energy Physics* **2008**, 100 (2008).
- [34] S. Cao and A. Majumder, Nuclear modification of leading hadrons and jets within a virtuality ordered parton shower, *Phys. Rev. C* **101**, 024903 (2020), [arXiv:1712.10055 \[nucl-th\]](#).
- [35] A. M. Sirunyan *et al.* (CMS), First measurement of large area jet transverse momentum spectra in heavy-ion collisions, *JHEP* **05**, 284, [arXiv:2102.13080 \[hep-ex\]](#).
- [36] T. Sjöstrand, The PYTHIA Event Generator: Past, Present and Future, *Comput. Phys. Commun.* **246**, 106910 (2020), [arXiv:1907.09874 \[hep-ph\]](#).
- [37] T. Sjöstrand and M. van Zijl, A multiple-interaction model for the event structure in hadron collisions, *Phys. Rev. D* **36**, 2019 (1987).
- [38] J. S. Moreland, J. E. Bernhard, and S. A. Bass, Alternative ansatz to wounded nucleon and binary collision scaling in high-energy nuclear collisions, *Phys. Rev. C* **92**, 011901 (2015), [arXiv:1412.4708 \[nucl-th\]](#).
- [39] V. Vovchenko, Cooper-frye sampling with short-range repulsion, *Physical Review C* **106**, 10.1103/physrevc.106.064906 (2022).
- [40] M. McNelis and U. Heinz, Modified equilibrium distributions for cooper-frye particlization, *Physical Review C* **103**, 10.1103/physrevc.103.064903 (2021).
- [41] J. Casalderrey-Solana, D. C. Gulhan, J. G. Milhano, D. Pablos, and K. Rajagopal, Angular structure of jet quenching within a hybrid strong/weak coupling model, *Journal of High Energy Physics* **2017**, 10.1007/jhep03(2017)135 (2017).
- [42] P. Huovinen and H. Petersen, Particlization in hybrid models, *The European Physical Journal A* **48**, 10.1140/epja/i2012-12171-9 (2012).
- [43] A. Majumder, Incorporating Space-Time Within Medium-Modified Jet Event Generators, *Phys. Rev. C* **88**, 014909 (2013), [arXiv:1301.5323 \[nucl-th\]](#).
- [44] F.-L. Liu, W.-J. Xing, X.-Y. Wu, G.-Y. Qin, S. Cao, and X.-N. Wang, QLBT: a linear Boltzmann transport model for heavy quarks in a quark-gluon plasma of quasi-particles, *Eur. Phys. J. C* **82**, 350 (2022), [arXiv:2107.11713 \[hep-ph\]](#).
- [45] Y. He, T. Luo, X.-N. Wang, and Y. Zhu, Linear Boltzmann Transport for Jet Propagation in the Quark-Gluon Plasma: Elastic Processes and Medium Recoil, *Phys. Rev. C* **91**, 054908 (2015), [Erratum: *Phys.Rev.C* 97, 019902 (2018)], [arXiv:1503.03313 \[nucl-th\]](#).
- [46] S. Cao, T. Luo, G.-Y. Qin, and X.-N. Wang, Linearized Boltzmann transport model for jet propagation in the

- quark-gluon plasma: Heavy quark evolution, *Phys. Rev. C* **94**, 014909 (2016), [arXiv:1605.06447 \[nucl-th\]](#).
- [47] S. Shi, R. Modarresi Yazdi, C. Gale, and S. Jeon, Comparing the MARTINI and CUJET models for jet-quenching: I. medium modification of jets and jet substructure, (2022), [arXiv:2212.05944 \[hep-ph\]](#).
- [48] R. M. Yazdi, S. Shi, C. Gale, and S. Jeon, Leading order, next-to-leading order, and nonperturbative parton collision kernels: Effects in static and evolving media, *Phys. Rev. C* **106**, 064902 (2022), [arXiv:2206.05855 \[hep-ph\]](#).
- [49] A. Kumar *et al.* (JETSCAPE), Inclusive Jet and Hadron Suppression in a Multi-Stage Approach, (2022), [arXiv:2204.01163 \[hep-ph\]](#).
- [50] Y. Hidaka and R. D. Pisarski, Hard thermal loops, to quadratic order, in the background of a spatial 't hooft loop, *Physical Review D* **80**, [10.1103/physrevd.80.036004](#) (2009).
- [51] N. Armesto, L. Cunqueiro, and C. A. Salgado, Q-PYTHIA: A Medium-modified implementation of final state radiation, *Eur. Phys. J. C* **63**, 679 (2009), [arXiv:0907.1014 \[hep-ph\]](#).
- [52] D. Acosta, T. Affolder, M. G. Albrow, and D. Ambrose (CDF Collaboration), Underlying event in hard interactions at the fermilab tevatron  $\bar{p}p$  collider, *Phys. Rev. D* **70**, 072002 (2004).
- [53] T. Affolder and H. Akimoto (CDF Collaboration), Charged jet evolution and the underlying event in proton-antiproton collisions at 1.8 tev, *Phys. Rev. D* **65**, 092002 (2002).
- [54] A. Kumar *et al.* (JETSCAPE), JETSCAPE framework:  $p + p$  results, *Phys. Rev. C* **102**, 054906 (2020), [arXiv:1910.05481 \[nucl-th\]](#).
- [55] D. Pablos, Jet suppression from a small to intermediate to large radius, *Physical Review Letters* **124**, [10.1103/physrevlett.124.052301](#) (2020).
- [56] I. Lokhtin, L. Malinina, S. Petrushanko, A. Snigirev, I. Arsene, and K. Tywoniuk, Heavy ion event generator HYDJET (HYDrodynamics plus JETs), *Computer Physics Communications* **180**, 779 (2009).
- [57] I. P. Lokhtin, A. V. Belyaev, and A. M. Snigirev, Jet quenching pattern at LHC in PYQUEN model, *The European Physical Journal C* **71**, [10.1140/epjc/s10052-011-1650-1](#) (2011).
- [58] C. Shen, Z. Qiu, H. Song, J. Bernhard, S. Bass, and U. Heinz, The iEBE-VISHNU code package for relativistic heavy-ion collisions, *Comput. Phys. Commun.* **199**, 61 (2016), [arXiv:1409.8164 \[nucl-th\]](#).